Using cell potential energy to model the dynamics of adhesive biological cells

Stephen Turner*
Center for Theoretical Modelling in Medicine, Department of Mathematics, Heriot-Watt University, Edinburgh EH14 4AS, Scotland
(Received 4 October 2004; published 7 April 2005)

Developing a continuous mathematical model of a physical phenomenon which is based on a discrete model of the same system is not straightforward. Yet such a process is useful in illustrating the link between the individual behavior of the elements comprising a system and its macroscopic behavior. Collections of biological cells can exhibit phenomena such as pattern formation, aggregation, and invasion, and mathematics has proven useful in elucidating the underlying dynamics of these phenomena. The continuous models formulated are frequently of reaction-diffusion form, and central to their application is a knowledge of the diffusion coefficient of a collection of the elements comprising the system. Cohen and Murray [J. Math Biol. **12**, 237 (1981)] developed a means of deriving this quantity which has since been largely neglected by model developers, and which is based on a knowledge of the potential energy associated with the mutual interaction between the cells. In this work, we begin by deriving the energy of interaction of biological cells modeled as adhesive, deformable spheres. In so doing, we are able to quantify the equilibrium density of a biological cell aggregate, and also obtain a quantitative estimate of the diffusion coefficient of a collection of cells modeled in this way. In so doing, we are able to use experimental data from single-cell studies of the adhesiveness and cell membrane elasticity of a biological cell to derive the diffusion coefficient of a cell mass composed of a collection of identical cells. This allows us to better inform the parameter values used in reaction-diffusion models of biological systems. We go on to apply this technique to a particular situation: modeling the dynamics of a collection of biological cells which experience strong cell-cell adhesion. In so doing, we derive a nonlinear fourth-order partial differential equation to model this system. We conclude by discussing the practical utility of this work in illuminating the link between the microscopic behavior of individual biological cells and the macroscopic behavior of the aggregate to which they give rise, and also by giving some insights into how the modeling of cell-cell adhesion may be treated mathematically.

DOI: 10.1103/PhysRevE.71.041903 PACS number(s): 87.18.Ed, 87.18.Hf, 87.18.La, 83.60.Df

I. INTRODUCTION

Mathematical modeling has produced a wealth of insight into the dynamics of biological phenomena, such as embryogenesis [2,3], tumor growth [4–10], population dynamics [11–13], and pattern formation [14–18]. These models can be continuous (formulated as sets of partial differential equations), discrete (where the elements are modeled as individual points moving on a lattice), or hybrid (a mixture of the previous two). Obviously, if we are modeling the same system, then we would expect all of the different modeling strategies to produce the same qualitative results. However, the process of basing a continuous model of a system (presumed to apply at length scales much greater than the size of the individual elements comprising it) upon a discrete model describing the same system has proven to be mathematically problematic, although there have been attempts [12,19,8,6,20,21].

In this paper, we take the work of Cohen and Murray [1] and Murray [22] and use it to make a contribution to this question. These workers demonstrated that, by formulating a "potential energy of interaction" between the elements comprising the system, one may obtain an estimate both of the particles' diffusion coefficent as well as the equilibrium density of the system. Frequently collections of motile, reactive biological cells are modeled using a reaction-diffusion equation such as the Fisher equation,

$$\frac{\partial n}{\partial t} = \frac{\partial}{\partial x}\left[D(n)\frac{\partial n}{\partial x}\right] + rn\left(1 - \frac{n}{K}\right), \tag{1}$$

where the first term on the right quantifies the motility of the cells, and the second their growth kinetics. In this case the logistic growth term is used. However, cell kinetics can be described in a variety of ways which are related to the competition which exists between proliferation and its inhibition due to both physiological and environmental factors [23], The parameters r and K determine the growth rate and equilibrium density of the cell mass. Clearly, an approach to modeling a biophysical system which allows us to take single-cell experimental data and use them to obtain the equilibrium density and diffusivity of a collection of such cells would be useful to have, since it would allow us to more accurately obtain these parameters for use in reaction-diffusion models. This is what the cell potential energy approach can yield.

Although this method of determining equilibrium density and diffusivity is novel in the biological context, it already has a long history of usefulness in the context of condensed matter theory. The processes of nucleation and condensation [24], phase separation [25], and spinodal decomposition [26,27] are modeled using an energy minimization approach such as that which we will describe here. These previous

*Email address: stephen@ma.hw.ac.uk

studies have relevance to biology: in the process of, for example, skeletal condensation in embryogenesis [28,29], evolving cells become increasingly adhesive over time giving rise to the formation of increasingly dense cellular aggregates which then differentiate into cartilage to form the precursor of the neonatal skeleton. Conversely, in oncology, it is known that as malignant cells mutate over time they become less and less adhesive, and hence more likely to break free from their neighbors and invade healthy tissue [30].

We begin in Sec. II by describing the mathematical background to the cell potential energy approach, and then considering how we may apply it to aggregates of biological cells. We make reference to the previous work of the author [6,31] in which the extended Potts model (an energy minimization technique) was usefully applied to the study of adhesive cell aggregates in the context of modeling malignant tumors. On the basis of this previous work, we explain how we may obtain an energy per unit length associated with adhesion, and an energy term to quantify the elastic potential energy of the cell membrane. We go on to argue that the continuous equivalent to modeling biological cells in the manner of the Potts model would be to approximate them as being adhesive, elastic spheres. On this basis, we obtain an expression for the energy of interaction between neighboring cells. In Sec. III, we present results in which we have determined quantitatively the equilibrium density of a cell aggregate in which the cells have been modeled in this way, and we use Cohen and Murray's approach to obtain quantitative estimates of the diffusion coefficient of a collection of such cells. In Sec. IV, we apply this technique to the modeling of a particular physical system: the dynamics of a collection of biological cells in which cell-cell adhesion is particularly significant. In so doing, we derive a fourth-order partial differential equation to describe this system. We conclude in Sec. V with a discussion of the utility of this approach.

II. THE MODEL: CELL POTENTIAL ENERGY AND DIFFUSIVITY

If we consider a collection of particles described by the density field $n(\mathbf{x},t)$, then the total energy of the system is defined to be the integral of the energy density taken over the domain,

$$E = \int_V e(n)\mathbf{dx}. \tag{2}$$

The chemical potential μ of a physical system is defined to be the change in the energy $E(n)$ of the system caused by a change in particle number,

$$\mu = \frac{\delta E}{\delta n} = e'(n). \tag{3}$$

Physical systems tend to reconfigure themselves such that their energy is minimized. Fick's law describes the movement of particles during this reconfiguration, and states that the flux of particles in a spatially inhomogeneous system is proportional to the gradient of the potential energy,

$$\mathbf{\Phi} = -D\,\boldsymbol{\nabla}\,\mu(n), \tag{4}$$

where D is a proportionality constant. Conservation of mass then gives us

$$\frac{\partial n}{\partial t} = -\,\boldsymbol{\nabla}\cdot\mathbf{\Phi} = \boldsymbol{\nabla}\cdot[D\,\boldsymbol{\nabla}\,\mu(n)]. \tag{5}$$

We may, therefore, write

$$D^*(n) = D\frac{\partial \mu}{\partial n} = De''(n) \tag{6}$$

hence

$$\frac{\partial n}{\partial t} = \boldsymbol{\nabla}[\alpha(n)\,\boldsymbol{\nabla}\,n], \tag{7}$$

where $\alpha(n)=D^*(n)$ is a density-dependent diffusion coefficient. Cohen and Murray [1] state that the energy density for an ensemble of noninteracting particles has the form

$$e(n) = \frac{1}{2}an^2 \tag{8}$$

(a result which can be derived from kinetic theory and the law of mass action): in this case, $D^*=aD$, a constant, and Eq. (7) becomes the familiar form of the diffusion equation with constant diffusion coefficient

$$\frac{\partial n}{\partial t} = D^*\boldsymbol{\nabla}^2 n. \tag{9}$$

The most important assumption in this derivation is that the energy density can be given by Eq. (8), which applies only to the noninteracting "ideal gas" situation. The most obvious point for us to begin, therefore, is to develop energy terms associated with cell-cell and cell-medium adhesiveness as well as cell membrane elasticity, and use these to develop a term for the energy density which is more general than the ideal-gas approximation, and which takes into account adhesive interactions between the cells as well as the cell membrane elasticity.

The extended Potts model has been usefully applied to the simulation of tumor growth and invasion [4,6,31], and uses an energy-minimization technique for biological cells modeled as discrete entities. In this model—which takes place on a square lattice—adjacent lattice points which have been given the same label σ are defined to lie in the same biological cell; see Fig. 1. Since the simulated cells are spatially extended, we are able to model accurately the adhesive energy per unit length of cell surface, as well as the elastic energy of the cell membrane. In our previous work, the energy associated with cell-cell adhesion is defined through an energy per unit length J_{cc}, whereas that associated with cell-medium adhesion is defined through J_{cm}. The energy associated with the cell membrane elasticity is defined to be $\lambda(v_\sigma - V_T)^2$, where λ is defined to be the coefficient of elasticity associated with the cell membrane, and V_T is the relaxation volume of the cell. By randomly selecting a lattice point, copying the parameters for it into a neighbor which does not lie within the same cell, applying the METROPOLIS algorithm,

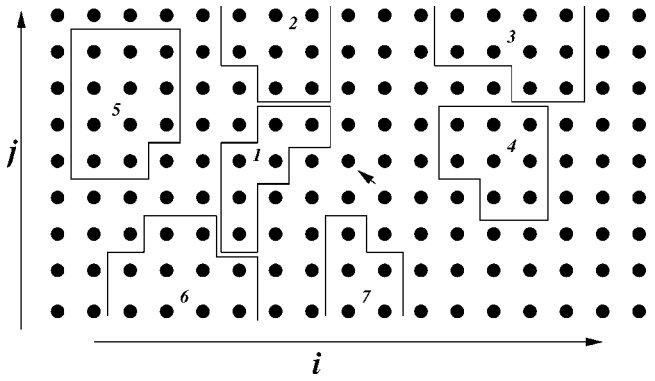

FIG. 1. How biological cells are simulated as being spatially extended entities in the Potts model. Neighboring lattice points with the same label are defined to lie within the same cell. Cells interact with the medium and their neighbors through adhesion, modeled as the energy per unit length of cell perimeter associated with the interaction. Changes in cell perimeter and volume give rise to deformation of the cell membrane, which is an elastic medium and has a mechanical energy of deformation associated with it. The system is evolved using a Monte Carlo simulation, and approaches the cellular configuration associated with the system's energy minimum.

and iterating, we are able to track the evolution of the system as it approaches its energy minimum. In this way, we are able to model the phenomenon of differential adhesion-driven sorting of motile biological cells, and we concentrated specifically on tumor growth. For further details, we refer the reader to our previous work [6].

Since the Potts model simulation takes place on a square lattice, the cells have an appearance which reflects the geometry of the square lattice. However, in the limit where the distance between lattice points tends to zero, the cell surface would become increasingly smooth and the discrete nature of the grid would become less and less apparent. In the limit, then, the cells would have a smooth surface. Isolated cells in an adhesive medium tend to be approximately spherical—and in the case of malignant cells, this spherical geometry becomes increasingly apparent as the cells continue to mutate. To a first approximation, therefore, in our continuous model we define the cells to be spherical and we work out the energy of adhesion and elasticity on this basis.

Consider the cell mass illustrated in Fig. 2, in which the cells have been modeled as adhesive, elastic spheres. In arriving at this configuration from complete separation ($\theta=0$), there has been an increase in cell-cell contact of ΔL_{cc} and a reduction of cell-medium contact of ΔL_{cm}. The potential energy of a single cell at this intercellular separation (neglecting the random motility for now) is given by

$$e_1 = J_{cc}\Delta L_{cc} - J_{cm}\Delta L_{cm} + \lambda(\Delta V)^2, \tag{10}$$

where the ΔL's are the change in the length of cell-cell or cell-medium contact in arriving at this density from complete separation, and the other terms are the same as defined for the Potts model (J_{cc} is the energy per unit length of cell-cell contact, J_{cm} is the energy per unit length of cell-medium contact, and λ is the cell membrane elasticity). This expression is the potential energy of a single cell in contact with its neighbors in the square configuration illustrated in Fig. 2. The energy density of an ensemble of particles interacting in this way will be given by the single cell energy multiplied by the number of particles per unit volume,

$$e(n) = ne_1 = n[J_{cc}\Delta L_{cc} - J_{cm}\Delta L_{cm} + \lambda(\Delta V)^2]. \tag{11}$$

For completeness, we add in the energy term from Eq. (8) and using Eq. (11) we see that the total energy density of the system is given by

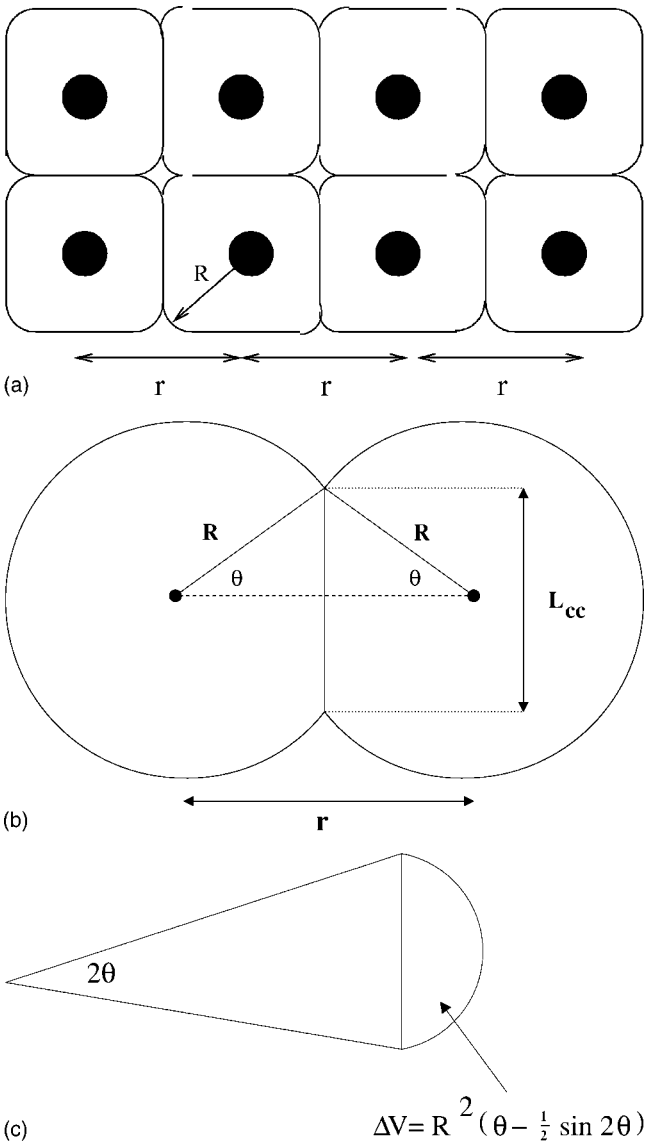

FIG. 2. If we model the cells as being deformable elastic spheres, then at high density they will be compressed to an equilibrium density dependent on the relative strengths of the coefficients of adhesiveness and elasticity. When cells come into contact, there is a change in the length of cell membrane which is in contact with the medium and with other cells, and there is also a change in volume, as illustrated. We can relate these changes to the intercellular spacing r and, by regarding the intercellular spacing as being proportional to the reciprocal of the density, we can work out ΔL_{cc}, ΔL_{cm}, and ΔV as functions of n.

$$e(n) = \frac{1}{2}an^2 + n[J_{cc}\Delta L_{cc} - J_{cm}\Delta L_{cm} + \lambda(\Delta V)^2]. \quad (12)$$

If we examine Fig. 2, we see that simple geometry gives us

$$\Delta L_{cc} = 8R \sin\theta, \quad (13)$$

$$\Delta L_{cm} = 8R\theta, \quad (14)$$

and

$$\Delta V = 4R^2\left(\theta - \frac{1}{2}\sin 2\theta\right), \quad (15)$$

where

$$\theta = \cos^{-1}\left(\frac{r}{2R}\right). \quad (16)$$

If we take the density to be proportional to the reciprocal of the intercellular spacing,

$$n = \frac{\kappa}{r}, \quad (17)$$

where κ is a constant, then we can write

$$\theta = \cos^{-1}\left(\frac{\kappa}{2Rn}\right), \quad (18)$$

therefore

$$e(n) = \frac{1}{2}an^2 + 8n\left[RJ_{cc}\sin\theta - RJ_{cm}\theta + 2R^4\lambda\left(\theta - \frac{1}{2}\sin 2\theta\right)^2\right]. \quad (19)$$

This expression quantifies the energy density of cells modeled in the way described. We now present results in which we have shown how this expression—containing parameters for single-cell adhesiveness and elasticity—can be used to derive the macroscopic equilibrium density and diffusion coefficient of a collection of these cells.

III. RESULTS

A. Equilibrium density and carrying capacity

Our interest is in the situation where cells are closely packed and adhesive. Figure 3 illustrates the form of the energy density $e(n)$ against density n for varying values of cell-cell and cell-medium adhesiveness, where we have set $a=0$. The range of n considered begins at $n=1/2R$, where R is the radius of one cell (set to three units in our study), and corresponds to the average density at which neighboring cells would just begin to touch, and, therefore, aggregate if they are sufficiently adhesive. As we mentioned earlier, Eq. (8) applies only to the ideal gas approximation, corresponding to a collection of particles interacting only through collisions with each other. In the situation which we are describing, this approximation is not appropriate as the cells have strong cell-cell and cell-medium adhesiveness; in addition, the membranes are elastic, which gives rise to a repulsive

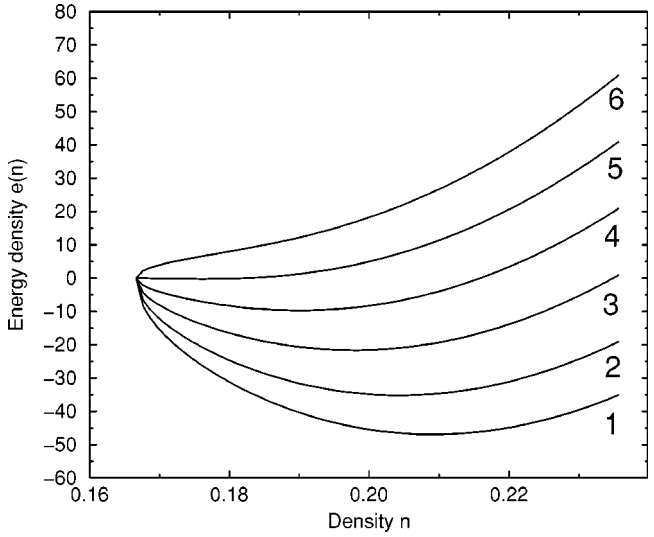

FIG. 3. The change in the energy density as the strength of cell-cell adhesion is changed: 1, strong cell-cell adhesion; 6, weak cell-cell adhesion. As we can see, the location of the energy minimum decreases as this strength is reduced until the energy minimum disappears when $J_{cm}=J_{cc}$. Notice also that when cell-cell adhesion is weaker than cell-medium adhesion, the minimum disappears, corresponding to it being energetically unfavorable for the cells to aggregate at all. [$a=0$, $\lambda=2$, $R=3$, $\kappa=1$ throughout. 1, $J_{cm}=20$, $J_{cc}=1$; 2, $J_{cm}=20$, $J_{cc}=5$; 3, $J_{cm}=20$, $J_{cc}=10$; 4, $J_{cm}=20$, $J_{cc}=15$; 5, $J_{cm}=20$, $J_{cc}=20$; 6, $J_{cm}=20$, $J_{cc}=25$.]

effect for high density. In addition, experimental evidence concerning the behavior of cell masses sorting under the influence of differential adhesion indicates that the effect of random motility is minor [32]. It seems a reasonable approximation, therefore, to neglect the effect of random motility for adhesive cells in close contact. This is the reason for our setting $a=0$ for $n>n_{\min}$, where $n_{\min}$ is the density at which the cells just begin to touch (on average).

As we can see from Fig. 3, when cell-cell adhesiveness is stronger than cell-medium adhesiveness, there is a local equilibrium at high density, and this is the density to which the system would relax. Notice that as the strength of cell-cell adhesiveness (relative to cell-medium adhesiveness) is increased, this minimum moves to higher density, corresponding to closer packing of the cells (as we would expect).

It will be remembered from our discussion in Sec. I that the spatially homogeneous equilibrium density of a cell mass modeled by the Fisher equation is defined by the carrying capacity K in Eq. (1). This parameter is usually thought to be determined by considerations such as nutrient and oxygen availability [8,33]. In previous studies of the Fisher equation, it has always been implicitly assumed that cell-cell adhesiveness is insufficiently strong to cause aggregation to occur, and that the equilibrium density of the cell mass is determined by these environmental factors. This is appropriate for biological cell aggregates in which cell-cell adhesion is weak (e.g., aggressive malignancies [30]). However, it is not appropriate for the situation where cell-cell adhesion is strong: for example, benign tumors, or embryological aggregates where progressive cell differentiation is accompanied by increased expression of cell surface adhesion molecules [28].

In these latter scenarios, it may well be the case that the carrying capacity is higher than the actual equilibrium density of the cell mass. Conversely, if the capacity of the environment to support cells is lower than the equilibrium density given from the analysis illustrated in Fig. 3, then it would be the case that cells would die through a lack of nourishment until the local density reduced sufficiently. Hence, when modeling cell masses in which adhesiveness is a significant factor, it is insufficient to determine K simply by considering only the implications of nutrient and oxygen availability. Taking these other factors into account would allow the development of more accurate reaction-diffusion models of these phenomena.

B. The diffusion coefficient

From our derivation in Sec. II, recall that the diffusion coefficient is proportional to the second derivative of the energy density—see Eq. (6). By taking two sets of parameter values, we evaluated the second derivative numerically to obtain the profiles illustrated in Fig. 4. In so doing, we obtained a diffusion coefficient D^* which depends on both cell density and the microscopic parameters of the Potts model. We see that D^* increases with cell-cell adhesiveness in the situation where aggregation can occur: this is due to rapid viscoelastic relaxation effects when cells are undergoing strongly attractive interactions with each other. If we recall the usual relationship between the flux $\mathbf{\Phi}$, the diffusion coefficient D, and the density gradient ∇n,

$$\mathbf{\Phi} = -D\nabla n, \tag{20}$$

we see that the diffusion coefficient is proportional to the ratio between the flux of particles and the density gradient. Close to the spatial separation at which two cells are very close to each other, a tiny change in their separation causing them to touch may give rise to a large change in flux, resulting in a large value of D at these separations.

Notice the divergence of the second derivative as the cells separate from each other [i.e., $\theta=0$ in Eq. (18)] and $n \rightarrow (\kappa/2R)^+ = 0.166^+$. This is not an artefact of the numerical differentiation. It is a consequence of the assumption of spherical symmetry, and of us concentrating on the energy change associated with two cells coming together rather than that associated with a large number of cells with a distribution of sizes and separations. In order to demonstrate that this divergence comes from the modeling and not the numerical differentiation, we have evaluated the second derivative of the energy density analytically, and shown that it diverges as $n \rightarrow (\kappa/2R)^+ = 0.166^+$: this derivation is given in Appendix A. This divergence is not of practical importance, however, for several reasons. First, the exact value of n at which the diffusion coefficient diverges would be smoothed out in reality for several reasons. Consider the particular case where $\kappa=1$ and the cell radius $R=3$: then the divergence occurs at $n = 1/2R = 0.166$. In reality, there will be a distribution of values of R (of around 10% on either side of this mean due to variations in osmotic pressure across the cell membrane), which will cause the location of the divergence to be smoothed out over a range of values. Second, the reason for the divergence mathematically is due to the divergence of the first derivative of $\cos^{-1}(\kappa/2Rn)$ as $n \rightarrow (\kappa/2R)$, which in turn comes from the assumption that the cells are completely spherically symmetric. In reality, the cells will have a distribution of shapes. Spherical symmetry is a reasonable approximation; however, when two real cells come into contact in the manner in which we have modeled here, adhesive effects at the point of touching may give rise to a rapid rate

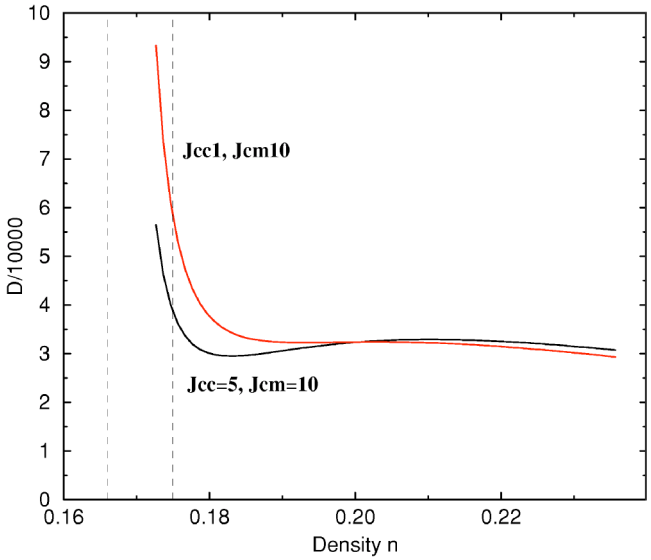

FIG. 4. The diffusion coefficient D vs density for two values of the adhesiveness coefficients, illustrating the second derivative of the energy density for two cases where cell-cell adhesion is stronger than cell-medium adhesion (and, hence, aggregation will occur). In keeping with Eq. (3), these curves correspond to the diffusion coefficient of the system [defined by Eq. (6)], which is in turn dependent on density, adhesiveness, and cell membrane elasticity. The leftmost dashed vertical line denotes the value of n at which D^* diverges. At the left of the graph—at densities close to the region in which the cells are touching, but only just—D^* is large. In the region enclosed by the dashed vertical lines, the fact that there is a distribution in cell size and shape has to be taken into account, as do the random fluctuations of the cell membrane. By using experimental evidence for the amplitude of these fluctuations, we estimate the minimum surface area of contact required before the cells can begin to relax towards their equilibrium separation: this is denoted in the figure by the rightmost vertical dashed line. We expect the flux of cells to be particularly high around this region, and the velocity of their movement towards each other to be particularly rapid. This can be understood by realizing that deviations from equilibrium will be smoothed out through a viscoelastic relaxation which will occur at a rate far greater than that of passive diffusion. Notice also that, around the same region of density, D^* is greater for the case of strongest cell-cell adhesiveness. This is because the gradient of the potential energy [corresponding to the *first* derivative of the energy density, see Eq. (3)] is greater for strong adhesiveness, as can be seen from an inspection of the curves in Fig. 3. Conversely, at high density, strongly adhesive cells have a lower D^* and, hence, will move more slowly for the same energy gradient compared with cells with weaker adhesion. This is because deviations from equilibrium are less energetically favorable as adhesiveness is increased (i.e., strongly adhesive cells are more difficult to move). ($a=0$, $\lambda=2$, $R=3$, $\kappa=1$ throughout.)

of relaxation towards their equilibrium separation. An *experimental* result intended to calculate D^* versus n would result in an *intersection* with the vertical axis in the region of $n=\kappa/(2R)$ rather than a divergence at it.

In addition to our assumptions concerning the size and shape of cells, we must also take into account the random fluctuations of the cell membrane. These are known collectively as "membrane ruffling" [32,34–36], and are the driving force behind differential adhesion-driven sorting. This random movement causes cell membranes to attach to and detach from each other over a small surface area and pull away in a random manner. These random movements of the membrane, caused by the expansion and contraction of the microtubules of the cytoskeleton, may pull apart the cells when the surface area of contact between them is low. Hence, even though the cells may be at a distance from each other corresponding (through $n=1/2r$) to a density *higher* than 0.166 in Fig. 4, the cells could detach from each other, and there would be no relaxation towards equilibrium. Hence, there would be a difference between the value of D^* predicted by the model and that which would actually occur when the surface area of contact is low. Fortunately, however, we can use experimental data to quantify this limitation. The likelihood of the cells coming together to above $n=1/2R$ but not relaxing towards equilibrium will be dependent on the strength and amplitude of this membrane ruffling, and on the strength of cell-cell and cell-medium adhesion. According to experiments on neural retinal and pigmented retinal chick cells, the amplitude of this random movement is at a maximum of $\sim$10% of the cell radius when the cells are suspended in saline, and significantly less when in an adhesive cellular aggregate [37,32]. Very extensive and elegant experimental work investigating the diffusion, deformation, and aggregation of *Hydra* cells supports this conclusion [38,39]. We can understand why the amplitude of these fluctuations goes down with increasing strength of adhesion in an aggregate by noting that when the membranes are adherent to each other, the "anchoring" effect would reduce the likelihood of the cytoskeleton being able to pull the membrane free from its neighbor; hence, the greater the surface area of contact between adhesive cells, the less likely it will be for the random fluctuations of the membrane to be able to pull the cells apart. If we take a generous estimate of these random fluctuations in the presence of adhesion as being around 5% of the cell radius, then the likely range of validity of the model for the set of parameter values used to generate Fig. 4 will begin at $n=0.175$ (as illustrated by the rightmost dashed vertical line on the graph). When the cells have a surface area of contact corresponding to this density, there will be little chance of a random fluctuation of the membrane causing the cells to detach.

To summarize, we have shown how the diffusion coefficient for a mass of interacting cells can be derived from cell potential energy considerations. We have derived an expression for the equilibrium energy density of a cell mass, and used this to obtain expressions for the diffusion coefficient and the equilibrium density which can be directly related to the Potts model parameters. As we will recall from our discussion of Eq. (1), this would be sufficient information for us to be able to set up and solve the Fisher equation: the equilibrium density would be equivalent to K,D would correspond to a density-dependent diffusion coefficient obtained from the second differential of the energy density, and r could be obtained either experimentally from measurements of the cells' mitotic rate or from clinical data concerning tumor doubling time. Since highly accurate measurements of single-cell adhesiveness and elasticity can be obtained from atomic force microscopy measurements, this allows us to develop reaction-diffusion models of biological cell dynamics which are informed by more accurate parameter values.

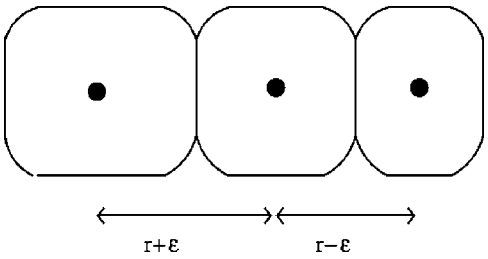

FIG. 5. When there is a spatial inhomogeneity in density present, the cells will deviate from their intercellular separation by an amount ϵ. By using a Taylor expansion on the resulting perturbation to the homogeneous energy, we can obtain an expression for the energy associated with the perturbation.

IV. MODELING THE DYNAMICS OF ADHESIVE BIOLOGICAL CELLS

In our derivation of the energy density of the system illustrated in Fig. 2, we assumed that the system was homogeneous; in other words, any spatial variation in density occurred over a length scale long compared to one cell diameter. This is a reasonable approximation when we are dealing with cell masses which are strongly adhesive to each other, as any long-range spatial inhomogeneity in density is likely to be quickly smoothed out through rapid viscoelastic relaxation. However, in the case of some biological situations in which the strength of cell-cell adhesion is significant, but not so strong as to produce a rapid relaxation to equilibrium (e.g., malignant cells from low-grade tumors), it may frequently be the case that such relaxation would be slow due to the reduced strength of cell-cell adhesion. This would give rise to variations in density over greater length scales, and in order for our model to be comprehensive we must take into account this situation. In this section, we model this situation, and obtan a nonlinear fourth-order partial differential equation to describe it.

Consider Fig. 5, which illustrates a cellular aggregate of the same type as that at the top of Fig. 2, but in this case the cells have undergone a deviation from their equilibrium separation. If we recall Eqs. (13)–(16), then we may write the resulting contributions to the energy from cell-cell adhesion, cell-medium adhesion, and cell membrane elasticity as follows, where we have used a Taylor expansion truncated at second order,

$$\Delta L_{cc} = 4R\sin\theta(n) + 2R\sin\theta(n-\epsilon_n) + 2R\sin\theta(n+\epsilon_n)$$
$$= 8R\sin\theta(n) + 2\epsilon_n^2 R\frac{\partial^2}{\partial n^2}[\sin\theta(n)], \qquad (21)$$

$$\Delta L_{cm} = 4R\theta(r) + 2R\theta(n+\epsilon_n) + 2R\theta(n-\epsilon_n)$$
$$= 8R\theta(n) + 2R\epsilon_n^2 \frac{\partial^2\theta(n)}{\partial n^2}, \tag{22}$$

$$\Delta V = 2R^2\left[\theta(n) - \frac{1}{2}\sin 2\theta(n)\right]$$
$$+ R^2\left[\theta(n+\epsilon_n) - \frac{1}{2}\sin 2\theta(n+\epsilon_n)\right]$$
$$+ R^2\left[\theta(n-\epsilon_n) - \frac{1}{2}\sin 2\theta(n-\epsilon_n)\right]$$
$$= 4R^2\left[\theta(n) - \frac{1}{2}\sin 2\theta(n)\right]$$
$$+ R^2\epsilon^2\left[\frac{\partial^2\theta(n)}{\partial n^2} - \frac{1}{2}\frac{\partial^2}{\partial n^2}[\sin 2\theta(n)]\right]. \tag{23}$$

Substituting Eqs. (21)–(23) into Eq. (10) and neglecting the ϵ_n^4 term, we obtain the following expression for the energy of a single cell in the configuration illustrated in the presence of spatial inhomogeneity in density,

$$e_{1(\mathrm{inh})} = e_{1(\mathrm{hom})} + \epsilon_n^2 h(n), \tag{24}$$

where

$$e_{1(\mathrm{hom})} = 8RJ_{cc}\sin\theta(n) - 8RJ_{cm}\theta(n)$$
$$+ 16R^4\lambda\left[\theta(n) - \frac{1}{2}\sin 2\theta(n)\right]^2 \tag{25}$$

and

$$h(n) = 2R\left[J_{cc}\frac{\partial^2}{\partial n^2}[\sin\theta(n)] - J_{cm}\frac{\partial^2\theta(n)}{\partial n^2} + 2R^3\lambda\right.$$
$$\left.\times[2\theta(n) - \sin 2\theta(n)]\left(\frac{\partial^2\theta(n)}{\partial n^2} - \frac{1}{2}\frac{\partial^2}{\partial n^2}[\sin 2\theta(n)]\right)\right]. \tag{26}$$

The parameter ϵ_n is the change in the (continuous) density field across one intercellular spacing r; hence, using Eq. (17) we may write

$$\epsilon_n = r\left(\frac{\partial n}{\partial x}\right) = \frac{\kappa}{n}\left(\frac{\partial n}{\partial x}\right). \tag{27}$$

The energy density of the system in the inhomogenous case is the energy of a single cell in this configuration multiplied by the number of cells per unit volume,

$$e_{\mathrm{inh}}(n) = ne_{1(\mathrm{inh})} = ne_{1(\mathrm{hom})} + n\epsilon_n^2 h(n), \tag{28}$$

and, since the chemical potential

$$\mu_{\mathrm{inh}} = e'_{\mathrm{inh}}(n) = \mu_{\mathrm{hom}} + \frac{d}{dn}[n\epsilon_n^2 h(n)], \tag{29}$$

we can take Eq. (29) and substitute it into Fick's equation

$$\mathbf{\Phi} = -D\nabla\mu \tag{30}$$

and use the continuity equation

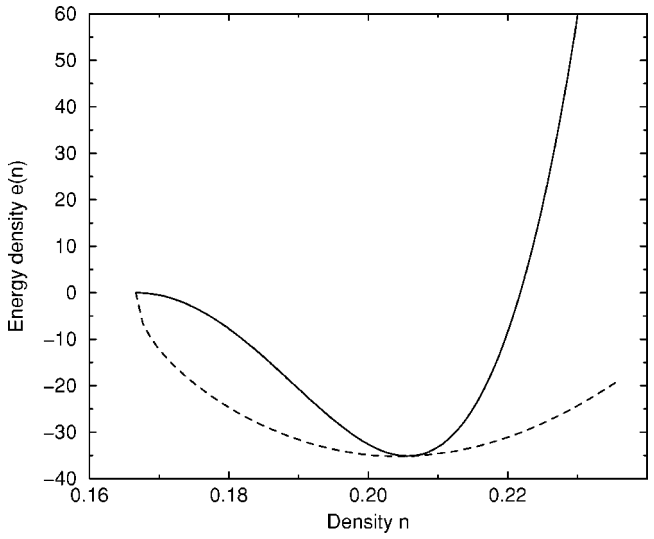

FIG. 6. The homogeneous energy density calculated from the deformable spheres model [dashed curve, Eq. (19)] compared with a fitted Landau-Ginzburg polynomial (solid curve) in the form of Eq. (34). The details of how the fit was conducted is described in the text. There is poor agreement far from equilibrium, but for small deviations from equilibrium the error is small. Using a fitted polynomial of Landau-Ginzburg type allows us to demonstrate the similarity between our analysis and previous work on aggregating systems, and permits the development of a fourth-order PDE to describe our model. (For the homogeneous energy: $J_{cc}=5$, $J_{cm}=20$, $\lambda=2$, $a=0$; fitted results: $A=-92\,423$, $B=60\,764\,946$.)

$$\frac{\partial n}{\partial t} = -\nabla\cdot\mathbf{\Phi} \tag{31}$$

to obtain

$$\frac{\partial n}{\partial t} = D\nabla^2\mu_{\mathrm{inh}} \tag{32}$$

$$= D\nabla^2\left(\mu_{\mathrm{hom}}(n) + \frac{d}{dn}[n\epsilon_n^2 h(n)]\right). \tag{33}$$

Clearly, taking Eq. (33) forward will require some simplification. We can gain some insight into how we may do this by considering the mathematical analysis of other physical systems which show aggregation (e.g., condensing gases, pinning in magnetic materials, and quenching of metal alloys [25–27]). In these cases, the homogeneous energy density is frequently approximated using the "Landau-Ginzburg" form

$$e_{\mathrm{hom}}(n) = \frac{An^2}{2} + \frac{Bn^4}{4}, \tag{34}$$

which, when $A<0$ and $B>0$, gives rise to a curve in the form of the solid line in Fig. 6. We proceed, therefore, by approximating the energy density of our system (illustrated as the dashed line in Fig. 6) with a polynomial of Landau-Ginzburg type, and approximating $h(n)$ with a linear polynomial. The latter assumption is reasonable for deviations around equilibrium, as illustrated in Fig. 7: the circles denote the equilibrium density.

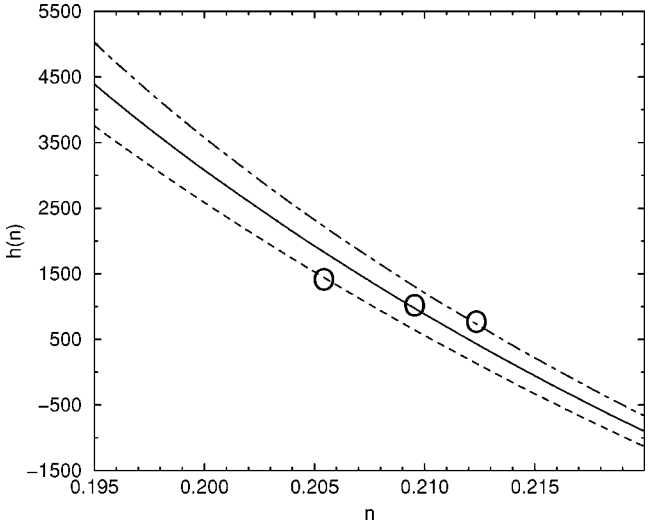

FIG. 7. $h(n)$ calculated from Eq. (26) plotted against density for varying adhesivenesses. The curves are plotted only for a range of densities close to their equilibrium values (denoted by the circles on the curves), as we have assumed that the deviation from equilibrium is not too great. As we can see, for small deviations around equilibrium $h(n)$ is approximately linear. [$\lambda=5$, $J_{cm}=20$ throughout; upper (dot-dashed) line $J_{cc}=8$; middle (solid) line $J_{cc}=10$; lower (dashed) line $J_{cc}=12$.]

The manner in which the fitting of the polynomial (34) to the form of the homogeneous energy density was conducted is described in detail in Appendix B. We insisted that the minima of both curves coincided (so that the equilibrium density was the same in both cases) and then selected values of A and B which minimized the mean error in the difference between the two curves. The reason for demanding that the minima of the two curves coincided was because both the simulated cells and their real-life counterparts are usually found close to their equilibrium densities. More specifically, if we define our fitted polynomial by the function

$$g(n) = \frac{A(n-n_{\min})^2}{2} + \frac{B(n-n_{\min})^4}{4}, \tag{35}$$

where $n_{\min}$ is the minimum value which the density can take while still allowing the cells to be in contact, then the equilibrium value n_{eq} can be evaluated as a function of A and B, which can in turn be evaluated through least-squares fitting.

Similarly, in the region around equilibrium as illustrated in Fig. 7, the $h(n)$ can reasonably be approximated using a linear function

$$h(n) \approx h_1 n + h_2, \tag{36}$$

where the coefficients h_1 and h_2 also can be obtained using least-squares fitting. By substituting Eqs. (36) and (35) into Eq. (29), we obtain

$$\mu_{\mathrm{inh}}(n) = [A(n-n_{\min}) + B(n-n_{\min})^3] + \frac{d}{dn}[n\epsilon_n^2(h_1 n + h_2)] \tag{37}$$

and by substituting this result into Eq. (33) and using Eq. (27), we obtain (for the 1D case)

$$\frac{\partial n}{\partial t} = D\frac{\partial^2}{\partial x^2}\left\{A(n-n_{\min}) + B(n-n_{\min})^3 + \frac{d}{dn}\left[\frac{\kappa^2}{n}\left(\frac{\partial n}{\partial x}\right)^2 (h_1 n + h_2)\right]\right\}. \tag{38}$$

In considering this highly nonlinear partial differential equation (PDE), we now review the established theory relating to condensing systems and investigate how our analysis relates to it.

If a system has spatial inhomogeneities in density, then Cahn and Hilliard demonstrated that the total energy of the nonequilibrium system may be written as the following perturbation to the equilibrium energy density:

$$E_{\mathrm{inh}}(n) = \int [E_{\mathrm{hom}}(n) + k(\nabla n)^2] d\mathrm{x}, \tag{39}$$

and, since

$$\mu(n) = \frac{dE}{dn}, \tag{40}$$

then

$$\mu_{\mathrm{inh}}(n) = \mu_{\mathrm{hom}}(n) + \frac{d}{dn}[k(\nabla n)^2], \tag{41}$$

where $\mu_{\mathrm{inh}}(n)$ is the chemical potential in the presence of spatial inhomogeneity. With this interpretation, the second term on the right quantifies the energy associated with inhomogeneities in density. By inspection of Eqs. (37) and (41) we see that there is a clear relationship between the inhomogeneous chemical potential as derived from our deformable spheres model and that derived from the Cahn-Hilliard equation. More specifically, we may write (in 1D)

$$\frac{d}{dn}\left[\frac{\kappa^2}{n}\left(\frac{\partial n}{\partial x}\right)^2 (h_1 n + h_2)\right] = \frac{d}{dn}\left[k\left(\frac{\partial n}{\partial x}\right)^2\right], \tag{42}$$

hence we may write

$$k = \frac{\kappa^2}{n}(h_1 n + h_2). \tag{43}$$

By inspection of Eq. (39), we see that k is equal to the energy associated with a squared unit of density gradient—which, in our analysis, is dependent on density. This is true in general [40,41]; however, Cohen and Murray [1] make the simplifying assumption that k is a constant which is independent of density, and deduce that

$$\mu_{\mathrm{inh}}(n) = \mu_{\mathrm{hom}}(n) - k\nabla^2 n = (An + Bn^3) - k\nabla^2 n, \tag{44}$$

which, using the continuity equation, gives rise to

$$\frac{\partial n}{\partial t} = D\nabla^2\mu_{\text{inh}}(n) = -k\nabla^4 n + A\nabla^2 n + B\nabla^2 n^3, \qquad (45)$$

which in 1D can be written

$$\frac{\partial n}{\partial t} = D\left[-k\frac{\partial^4 n}{\partial x^2} + (A + 3Bn^2)\frac{\partial^2 n}{\partial x^2} + 6Bn\left(\frac{\partial n}{\partial x}\right)^2\right]. \qquad (46)$$

If we include a logistical growth term $rn[1-(n/K)]$, then we obtain the following expression to describe the evolution of the system:

$$\frac{\partial n}{\partial t} = D\left[-k\frac{\partial^4 n}{\partial x^2} + (A + 3Bn^2)\frac{\partial^2 n}{\partial x^2} + 6Bn\left(\frac{\partial n}{\partial x}\right)^2\right] + rn\left(1 - \frac{n}{K}\right). \qquad (47)$$

The above equation has been studied analytically by Cohen and Murray [1], who performed a stability analysis which revealed stable solutions for $A<0$. Gourlay [42], also adding the same growth term, showed that it admits traveling-wave solutions. Fourth-order PDE's similar to Eq. (47) have been used to describe the behavior of aggregation in other physical systems, such as nucleation in metal alloys [27], spinodal decomposition [26], ecology and embryology [43–45], striations in chemical reactions [46], and in other areas of condensed-matter theory. Our work suggests that an equation with some aspects of similarity to Eq. (47) is also appropriate to modeling populations of cells with significant cell-cell adhesion.

To summarize, in our discussion we have shown how the diffusion coefficient for a mass of interacting cells can be derived from cell potential energy considerations. We have derived an expression for the equilibrium energy density of a cell mass, and used this to obtain expressions for the diffusion coefficient and the equilibrium density which can be directly related to the Potts model parameters. As we will recall from our discussion of Eq. (1), this would be sufficient information for us to be able to set up and solve the equation: the equilibrium density would be equivalent to K, D would correspond to a density-dependent diffusion coefficient obtained from the second differential of the energy density, and r could be obtained either experimentally from measurements of the cells' mitotic rate or from clinical data concerning tumor doubling time. We went on to take our deformable spheres model and introduced a spatial perturbation to it which provided us with a nonlinear equation to describe the situation where there are attractive interactions between the cells giving rise to spatial heterogeneities over length scales significantly greater than the radius of one cell diameter. In so doing, and applying the simplification that the homogeneous energy density associated with our model can be approximated by an energy function of Landau-Ginzburg type, we obtained a highly nonlinear PDE [Eq. (38)] which would represent a major challenge to solve. We have also been able to relate our work to that of previous authors who have studied aggregating and condensing physical systems. We were able to show some aspects of similarity between our equation and that obtained by these previous authors, and concluded that a PDE of the form (38) is the most likely way in which the influence of cell-cell adhesion could be included in a continuous model of cancer invasion.

V. DISCUSSION

It has been our objective in this work to form a bridge between discrete models of biophysical phenomena—the parameters for which involve single-cell measurements—and continuous models, which require measurements of macroscopic quantities such as diffusion coefficient and equilibrium density. By modeling biological cells as being adhesive, deformable spheres, we have been able to evaluate an energy density of a collection of such cells, and from this we have been able to work out these macroscopic quantities.

The expression for equilibrium density which we have developed determines the carrying capacity for a cell mass in the situation where nutrient and oxygen availability is good and cell-cell adhesiveness is strong, as under these circumstances the equilibrium density will be determined by the mechanical and adhesive properties of the cells themselves. This situation is common in embryological development [28], but would apply also to the proliferating rim of a spheroid close to a major blood vessel, or to a vascularized tumor composed of moderately adhesive cells (e.g., colorectal carcinoma [47]). The determination of this equilibrium density is of clinical significance, as the density of a tumor determines the dosage of radio- or chemotherapy which a patient would require in order to reduce the tumor load. It is known experimentally that the adhesive properties of a tumor are determined genetically, and correlate with the expression of cell surface molecules (such as E-cadherin) which are related to cell-cell and cell-medium adhesion. This expression varies between tumor types, so the equilibrium density also would vary between types—which is part of the reason why high-density solid tumors are more difficult to treat, and have a poorer prognosis. By developing a means of relating together the single-cell adhesive characteristics and the macrocopic equilibrium density, we have shed some light on how the molecular biology of genetic mutation can be related to the large-scale morphology and density of solid tumors.

In deriving an expression for the diffusion coefficient which is based on single-cell measurements of adhesion and elasticity, we have also been able to link together the microscopic and macroscopic behavior of a system. These parameters can be evaluated through the process of atomic force microscopy [48–50], and would allow us to provide more accurate values for the diffusion coefficients of collections of biological cells, which would in turn result in more accurate reaction-diffusion models of these systems. Hence, once again this work can be shown to be useful in linking together discrete and continuous models of a system.

Finally, we were able to relate the cell potential energy approach to the mathematical models used to describe condensation and aggregation in other physical systems. In so doing, we were able to derive a fourth-order partial differential equation, simplifications of which have been studied analytically [1,42,43] and which is likely to provide a compre-

hensive model of the dynamics of biological cells in which the strength of cell-cell adhesion is significant.

ACKNOWLEDGMENTS

S.T. thanks the EPSRC for financial support. Thanks also to Jonathan Sherratt for useful discussions.

APPENDIX A

In order to demonstrate that the divergence of the curves in Fig. 4 is a consequence of the model and not the numerical differentiation, we evaluate here the second derivative of the energy density analytically, and show that it diverges as $n \rightarrow 0.166^{+}$.

If we write Eq. (19) in the following form:

$$e(n) = \frac{1}{2}an^2 + 8n\mathcal{Z}, \tag{A1}$$

where

$$\mathcal{Z} = \left[RJ_{cc}\sin\theta - RJ_{cm}\theta + 2R^4\lambda\left(\theta - \frac{1}{2}\sin 2\theta\right)^2\right], \tag{A2}$$

then

$$\frac{\partial^2 e(n)}{\partial n^2} = a + 16\left(\frac{\partial \mathcal{Z}}{\partial n}\right) + 8n\left(\frac{\partial^2 \mathcal{Z}}{\partial n^2}\right). \tag{A3}$$

It can be shown that

$$\frac{\partial \mathcal{Z}}{\partial n} = \left(\frac{\partial \theta}{\partial n}\right)\left[RJ_{cc}\cos\theta - RJ_{cm} + 4R^4\lambda\left(\theta - \frac{1}{2}\sin 2\theta\right)(1-\cos 2\theta)\right] \tag{A4}$$

and

$$\frac{\partial^2 \mathcal{Z}}{\partial n^2} = \left(\frac{\partial^2 \theta}{\partial n^2}\right)\left[RJ_{cc}\cos\theta - RJ_{cm} + 4R^4\lambda\left(\theta - \frac{1}{2}\sin 2\theta\right)(1-\cos 2\theta)\right] + R\left(\frac{\partial \theta}{\partial n}\right)^2\left\{ -J_{cc}\sin\theta + 4R^3\lambda\left[(1-\cos 2\theta)^2 + 2\sin 2\theta\left(\theta - \frac{1}{2}\sin 2\theta\right)\right]\right\}. \tag{A5}$$

We are interested in the behavior of Eq. (A3) as we approach $n=\kappa/2R$ from above; hence, we must evaluate the limits

$$\lim_{n\rightarrow(\kappa/2R)^+}\left(\frac{\partial \mathcal{Z}}{\partial n}\right) = R(J_{cc}-J_{cm})\left\{\lim_{n\rightarrow(\kappa/2R)^+}\left(\frac{\partial \theta}{\partial n}\right)\right\} \tag{A6}$$

and

$$\lim_{n\rightarrow(\kappa/2R)^+}\left(\frac{\partial^2 \mathcal{Z}}{\partial n^2}\right) = R(J_{cc}-J_{cm})\left\{\lim_{n\rightarrow(\kappa/2R)^+}\left(\frac{\partial^2 \theta}{\partial n^2}\right)\right\}. \tag{A7}$$

If we introduce a change of variable

$$\zeta = \frac{\kappa}{2Rn} \tag{A8}$$

so that

$$\theta = \cos^{-1}\left(\frac{\kappa}{2Rn}\right) \equiv \cos^{-1}(\zeta), \tag{A9}$$

then

$$\frac{\partial \theta}{\partial n} = -\frac{2R\zeta^2}{\kappa}\left(\frac{\partial \theta}{\partial \zeta}\right) \tag{A10}$$

and

$$\frac{\partial^2 \theta}{\partial n^2} = \frac{4R^2\zeta^2}{\kappa^2}\left[2\left(\frac{\partial \theta}{\partial \zeta}\right) + \zeta^2\left(\frac{\partial^2 \theta}{\partial \zeta^2}\right)\right]. \tag{A11}$$

Our interest is in establishing the behavior of Eqs. (A10) and (A11) as ζ approaches 1 from below. In the region of $\zeta=1$, we can use the Taylor expansion

$$\theta(\zeta) \simeq \theta(1) + (\zeta-1)\left(\frac{\partial \theta}{\partial \zeta}\right) \tag{A12}$$

and note that

$$\frac{\partial \theta}{\partial \zeta} = \frac{-1}{\sqrt{(1-\zeta^2)}} \tag{A13}$$

to obtain

$$\theta(\zeta) \simeq \left(\frac{1-\zeta}{1+\zeta}\right)^{1/2} \tag{A14}$$

for $\zeta \simeq 1^{-}$. Using this result, we can show that

$$\frac{\partial \theta}{\partial \zeta} = \frac{1}{2}(1+\zeta)^{-1/2}(1-\zeta)^{-1/2}[-1-(1-\zeta)(1+\zeta)^{-1}] \tag{A15}$$

and

$$\frac{\partial^2 \theta}{\partial \zeta^2} = \frac{1}{4}[-1-(1-\zeta)(1+\zeta)^{-1}]\{(1-\zeta)^{-3/2}(1+\zeta)^{-1/2} - (1-\zeta)^{-1/2}(1+\zeta)^{-3/2}\} + \frac{1}{2}(1+\zeta)^{-1/2}(1-\zeta)^{-1/2}\{(1+\zeta)^{-1} + (1-\zeta)(1+\zeta)^{-2}\} \tag{A16}$$

both of which are divergent as $\zeta \rightarrow 1^{-}$. We conclude from this, therefore, that the derivatives in Eqs. (A6) and (A7) are also divergent, and that this result is due to our assumption that $\theta=\cos^{-1}(\kappa/2Rn)$, which in turn comes from our assumption of spherical symmetry.

APPENDIX B

If we define our fitted polynomial by the function

$$g(n) = \frac{A(n - n_{\min})^2}{2} + \frac{B(n - n_{\min})^4}{4}, \tag{B1}$$

where $n_{\min}$ is the minimum value which the density can take while still allowing the cells to be in contact, then the equilibrium value

$$g'(n_{\text{eq}}) = A(n_{\text{eq}} - n_{\min}) + B(n_{\text{eq}} - n_{\min})^3 = 0. \tag{B2}$$

Clearly, this equation has a trivial minimum at $n = n_{\min}$ and another corresponding to the high-density equilibrium. Substituting this value for A which we obtain from this into Eq. (B1), we obtain

$$g(n_{\text{eq}}) = -\frac{1}{4}B(n_{\text{eq}} - n_{\min})^4. \tag{B3}$$

If we evaluate $g(n_{\text{eq}})$ using the deformable spheres model [using Eq. (19) with suitable parameter values], then we can work out B using Eq. (B3) and A using Eq. (B2). Notice that, from Eq. (B2), the location of the minimum is given by

$$n_{\text{eq}} = n_{\min} + \sqrt{-A/B}. \tag{B4}$$

Hence, the position of the minimum is determined not by the absolute values of A and B but by their ratio A/B.

In order to work out the values of A and B which minimized the fitting error, we defined a fractional error for each data point,

$$\epsilon(n_i) = \frac{g(n_i) - e(n_i)}{e(n_i)}, \tag{B5}$$

where $g(n_i)$ is given by Eq. (B1) and $e(n_i)$ is the energy density evaluated at n_i using the deformable spheres model [see Eq. (19)]. We then selected values of A and B which kept the ratio A/B the same, but which minimized

$$\overline{\epsilon} = \frac{1}{N}\sum_{i=0}^{N}\left(\frac{\left|\frac{A(n_i - n_{\min})^2}{2} + \frac{B(n_i - n_{\min})^4}{4} - e(n_i)\right|}{e(n_i)}\right), \tag{B6}$$

where N is the number of data points.

[1] D. S. Cohen and J. D. Murray, J. Math. Biol. **12**, 237 (1981).
[2] K. M. Page, P. K. Maini, N. A. M. Monk, and C. D. Stern, J. Theor. Biol. **208**, 419 (2001).
[3] K. J. Painter, P. K. Maini, and H. G. Othmer, Bull. Math. Biol. **62**, 501 (2000).
[4] E. L. Stott, N. F. Britton, J. A. Glazier, and M. Zajaz, Math. Comput. Modell. **30**, 183 (1999).
[5] A. A. Patel, E. T. Gawlinski, S. K. Lemieux, and R. A. Gatenby, J. Theor. Biol. **213**, 315 (2001).
[6] S. Turner and J. A. Sherratt, J. Theor. Biol. **216**, 85 (2002).
[7] J. A. Sherratt and M. A. J. Chaplain, J. Math. Biol. **43**, 291 (2001).
[8] A. R. A. Anderson and M. A. J. Chaplain, Bull. Math. Biol. **60**, 857 (1998).
[9] R. A. Gatenby, P. K. Maini, and E. T. Gawlinski, Appl. Math. Lett. **15**, 339 (2002).
[10] H. M. Byrne and M. A. J. Chaplain, Math. Comput. Modell. **24**, 1 (1996).
[11] D. J. T. Sumpter and D. S. Broomhead, Proc. R. Soc. London, Ser. B **268**, 925 (2001).
[12] P. Turchin, J. Anim. Ecol. **58**, 75 (1989).
[13] A. Johansson and D. J. T. Sumpter, Theor Popul. Biol. **64**, 497 (2003).
[14] K. M. Page, P. K. Maini, and N. A. M. Monk, Physica D **181**, 80 (2003).
[15] K. J. Painter, P. K. Maini, and H. G. Othmer, Proc. Natl. Acad. Sci. U.S.A. **96**, 5549 (1999).
[16] K. P. Painter, P. K. Maini, and H. G. Othmer, J. Math. Biol. **41**, 285 (2000).
[17] M. R. Owen and J. A. Sherratt, J. Theor. Biol. **189**, 63 (1997).
[18] T. Sekimura, M. Zhu, J. Cook, P. K. Maini, and J. D. Murray, Bull. Math. Biol. **61**, 807 (1999).
[19] A. Deutsch and A. T. Lawniczak, Math. Biosci. **156**, 255 (1999).
[20] S. Turner, J. A. Sherratt, K. J. Painter, and N. J. Savill, Phys. Rev. E **69**, 021910 (2004).
[21] A. T. Lawniczak, Transp. Theory Stat. Phys. **29**, 261 (2000).
[22] J. D. Murray, *Mathematical Biology*, 2nd ed. (Springer-Verlag, Berlin, 1993).
[23] J. C. M. Mombach and N. Lemke, Europhys. Lett. **59**, 923 (2002).
[24] L. Granasy, Solid State Phenom. **56**, 67 (1997).
[25] E. Coutsias and B. A. Huberman, Phys. Rev. B **24**, 2592 (1981).
[26] J. W. Cahn, Trans. Metall. Soc. AIME **242**, 166 (1968).
[27] J. W. Cahn, Acta Metall. **14**, 1685 (1966).
[28] B. K. Hall and T. Miyake, Anat. Embryol. **186**, 107 (1992).
[29] B. K. Hall and T. Miyake, BioEssays **22**, 138 (2000).
[30] W. G. Stetler-Stevenson, S. Aznavoorian, and L. A. Liotta, "Tumor cell interactions with the extracellular matrix during invasion and metastasis," Annu. Rev. Cell Biol. **9**:541, 1993.
[31] S. Turner, J. A. Sherratt, and D. Cameron, J. Theor. Biol. **229**, 101 (2004).
[32] J. C. M. Mombach, J. A. Glazier, R. C. Raphael, and M. Zajaz, Phys. Rev. Lett. **75**, 2244 (1995).
[33] J. A. Sherratt, SIAM J. Appl. Math. **60**, 392 (2000).
[34] J. C. M. Mombach, Phys. Rev. E **59**, R3827 (1999).
[35] J. C. M. Mombach and J. A. Glazier, Phys. Rev. Lett. **76**, 3032 (1996).
[36] M. S. Steinberg and R. S. Foty, J. Cell Physiol. **173**, 135 (1997).
[37] P. B. Armstrong and D. Parenti, J. Cell Biol. **55**, 660 (1972).
[38] J. P. Rieu, A. Upadhyaya, J. A. Glazier, N. B. Ouchi, and Y. Sawada, Biophys. J. **79**, 1903 (2000).

[39] J. P. Rieu and Y. Sawada, Eur. Phys. J. B **27**, 167 (2002).
[40] J. S. Rowlinson, J. Stat. Phys. **20**, 197 (1979).
[41] O. Penrose (private communication).
[42] S. A. Gourlay and M. V. Bartucelli, Dyn. Stab. Syst. **15**, 253 (2000).
[43] F. Lara-Ochoa and V. P. Bustos, BioSystems **24**, 223 (1990).
[44] F. Lara Ochoa and J. D. Murray, Bull. Math. Biol. **45**, 917 (1983).
[45] F. Lara-Ochoa, BioSystems **17**, 35 (1984).
[46] B. A. Huberman, J. Chem. Phys. **65**, 2013 (1976).
[47] K. Nabeshima, T. Inoue, Y. Shimao, H. Kataoka, and M. Koono, Histol. Histopathol **14**, 1183 (1999).
[48] J. Guck, R. Ananthakrishnan, C. C. Cunningham, and J. Kas, J. Phys.: Condens. Matter **14**, 4843 (2002).
[49] J. Guck, R. Ananthakrishnan, H. Mahmood, T. J. Moon, C. C. Cunningham, and J. Kas, Biophys. J. **81**, 767 (2001).
[50] M. Benoit, D. Gabriel, G. Gerisch, and H. E. Gaub, Nat. Cell Biol. **2**, 313 (2000).